Published in final edited form as:
Int J Radiat Oncol Biol Phys. 2012 July 1; 83(3): e417–e422. doi:10.1016/j.ijrobp.2011.12.074.

Impact of heterogeneity-based dose calculation using a deterministic grid-based Boltzmann equation solver for intracavitary brachytherapy

Justin K. Mikell, B.S.[*,††], **Ann H. Klopp, M.D., Ph.D.**[††], **Graciela M. N. Gonzalez, MPH**[§], **Kelly D. Kisling, M.S.**[‖,††], **Michael J. Price, Ph.D.**[¶], **Paula A. Berner, B.S**[*], **Patricia J. Eifel, M.D.**[††], and **and Firas Mourtada, Ph.D.**[‖,#,§§]

[*]Department of Radiation Physics, The University of Texas MD Anderson Cancer Center, Houston, TX, USA

[††]Department of Radiation Oncology, The University of Texas MD Anderson Cancer Center, Houston, TX, USA

[§]Department of Biostatistics, The University of Texas MD Anderson Cancer Center, Houston, TX, USA

[‖]Department of Radiation Physics—Patient Care, The University of Texas MD Anderson Cancer Center, Houston, TX, USA

[#]Department of Experimental Diagnostic Imaging, The University of Texas MD Anderson Cancer Center, Houston, TX, USA

[†]The University of Texas Graduate School of Biomedical Sciences at Houston, Houston, TX, USA

[¶]Department of Physics and Astronomy, Louisiana State University and Agricultural & Mechanical College, Baton Rouge, LA, USA, and Mary Bird Perkins Cancer Center, Baton Rouge, LA, USA

[§§]Department of Radiation Oncology, Helen F. Graham Cancer Center, Newark DE, USA

Abstract

Purpose—To investigate the dosimetric impact of the heterogeneity dose calculation Acuros, a grid-based Boltzmann equation solver (GBBS), for brachytherapy in a cohort of cervical cancer patients.

Methods and Materials—The impact of heterogeneities was retrospectively assessed in treatment plans for 26 patients who had previously received ^{192}Ir intracavitary brachytherapy for cervical cancer with computed tomography (CT)/magnetic resonance (MR)-compatible tandems and unshielded colpostats. The GBBS models sources, patient boundaries, applicators, and tissue heterogeneities. Multiple GBBS calculations were performed: with and without solid model applicator, with and without overriding the patient contour to 1g/cc muscle, and with and without overriding contrast materials to muscle or 2.25 g/cc bone. Impact of source and boundary

Reprint requests to: Firas Mourtada, Ph.D., Helen F. Graham Cancer Center, Rm 1152, Newark, DE 19713. Tel: (302) 623-4691; Fax: (302) 623-4547; fmourtad@christianacare.org.

Conflict of Interest Notification: Conflicts of interest do not exist for the authors.

modeling, applicator, tissue heterogeneities, and sensitivity of CT-to-material mapping of contrast were derived from the multiple calculations. TG-43 and the GBBS were compared for the following clinical dosimetric parameters: Manchester points A and B, ICRU report #38 rectal and bladder points, three and nine o'clock, and D_{2cc} to the bladder, rectum, and sigmoid.

Results—Points A, B, D_{2cc} bladder, ICRU bladder, and three and nine o'clock were within 5% of TG-43 for all GBBS calculations. The source and boundary and applicator account for most of the differences between the GBBS and TG-43. The D_{2cc} rectum (n=3), D_{2cc} sigmoid (n=1), and ICRU rectum (n=6) had differences > 5% from TG-43 for the worst case incorrect mapping of contrast to bone. Clinical dosimetric parameters were within 5% of TG-43 when rectal and balloon contrast mapped to bone and radiopaque packing was not overridden.

Conclusions—The GBBS has minimal impact on clinical parameters for this cohort of GYN patients with unshielded applicators. The incorrect mapping of rectal and balloon contrast does not have a significant impact on clinical parameters. Rectal parameters may be sensitive to the mapping of radiopaque packing.

Keywords

brachytherapy; intracavitary; ^{192}Ir; grid-based Boltzmann solver; TG-43

INTRODUCTION

Intracavitary brachytherapy (ICBT) combined with external-beam radiotherapy is effective against cervical cancer. Much of the success with ICBT to date has been with two-dimensional (2D) treatment planning, but over the last decade, there has been a shift toward three-dimensional (3D) treatment planning (1). An advantage of 3D treatment planning for ICBT is the use of dose-volume histogram (DVH) parameters in dose-response modeling, as has been done in external beam radiotherapy.

Heterogeneity corrections are now the standard approach for external beam treatment planning, but there is currently no accepted treatment planning system (TPS) for brachytherapy that incorporates tissue heterogeneities. Heterogeneity calculations may significantly improve the accuracy of TPSs because they can compensate for air in the bowel, applicator materials, and patient boundaries. Current brachytherapy dose calculations are based on a single source dose distribution in water that is represented in the TPS by specific parameters (defined in the American Association of Physicists in Medicine Task Group 43 (TG-43) guidelines (2)).

Heterogeneities in brachytherapy have been studied by several groups. Poon *et al.* (3) used Monte Carlo (MC) simulations for high-dose-rate (HDR) endorectal brachytherapy to account for shielding, heterogeneities, and patient boundaries. Richardson *et al.* (4) studied the impact of air gaps around vaginal cylinders in patients. A recent phantom study reported by Kwan *et al.* indicated that the dose to the anterior wall of an empty (air-filled) rectum was 13% lower than dose to the same site in a material-filled one (5). More basic studies have evaluated the effects of applicator materials (6), tissue heterogeneities (5, 7, 8), and boundary conditions (9). To optimize cervical cancer brachytherapy, there is a need for 3D image-based treatment planning that accounts for the effects of applicators and tissue heterogeneities on dose distributions (10).

Recently, a grid-based Boltzmann equation solver (GBBS), Acuros, was developed specifically to perform accurate and rapid dose calculations for radiation therapy. For brachytherapy, Acuros solves the Boltzmann radiation transport equation for photons on a locally adaptive Cartesian grid. A commercial TPS with a GBBS is now available for use

with a number of ^{192}Ir sources. There have been studies on the details of this commercial GBBS (11-13) and its parent code applied to brachytherapy (14, 15). The purpose of this work was to retrospectively apply the commercial GBBS, which models sources, patient boundaries, applicator materials, and tissue heterogeneities to estimate doses for cervical cancer patients and compare these doses to standard TG-43 estimates.

METHODS AND MATERIALS

Patients

Twenty-six patients, who received ^{192}Ir HDR ICBT with CT/MR tandem and colpostat applicators in addition to external-beam radiotherapy for cervical cancer, were selected from a database at X X X Cancer Center. This retrospective dosimetric analysis was conducted under The X X X X X Cancer Center Institutional Review Board-approved chart review protocol.

All patients had a Foley balloon inserted into the bladder that was inflated with a 7:93 (vol/vol) mixture of iodinated contrast:water. Seventeen patients had contrast deposited using a rectal tube. Radiopaque gauze was wetted and packed inferiorly and superiorly to the colpostats to displace the anterior wall of the rectum and posterior wall of the bladder away from the high-dose region during treatment. Specifications of the rectal and packing contrast were unavailable.

Contouring

*C*ontours were delineated by a physician (X) at X X for the retrospective analysis. The rectum (n = 26), bladder (n = 26), and sigmoid (n = 23) were contoured to include the full thickness of the wall of each organ. The rectum was contoured from 1 cm above the anus to the sigmoid flexure. The sigmoid was contoured from the rectosigmoid flexure to the point at which the sigmoid extended into the anterior pelvis at the level of the pubic symphysis. The bladder was contoured superiorly from the urethra. Rectal contrast, foley balloon, and radiopaque packing were contoured by a physicist (X).

Treatment planning

The TPS used in the retrospective analysis was BrachyVision v8.8 (Varian Medical Systems, Palo Alto, CA). It includes both TG-43 and the GBBS Acuros v1.3.1 (Transpire Inc., Gig Harbor, WA). The GBBS source model was the HDR ^{192}Ir VS2000 (12, 16) with a 1-mm cable. The TPS includes a library of applicators represented as solid models. The computed tomography (CT)/magnetic resonance (MR) compatible applicators (#AL13030000, Varian Medical Systems, Palo Alto, CA) were selected from the library; these are unshielded applicators composed of Titanium with acetal caps.

The solid model applicators were manually registered to the planning CT. During transport the GBBS substitutes the applicator model and materials in place of the corresponding CT voxels. GBBS uses CT data outside of the applicators to account for tissue heterogeneities and patient boundaries.

The materials available for CT-to-material mapping and the densities that map to them include air (0.001 g/cc, 0.131 g/cc), lung (0.131 g/cc, 0.605 g/cc), adipose (0.605 g/cc, 0.985 g/cc), muscle (0.985 g/cc, 1.075 g/cc), cartilage (1.075 g/cc, 1.475 g/cc), bone (1.475 g/cc, 2.275 g/cc), Aluminum (2.275 g/cc, 3.560 g/cc) , Titanium (3.560 g/cc, 6.210 g/cc), and stainless steel (6.210 g/cc, 8.000 g/cc); attenuating contrast materials (iodine, barium sulfate) are not available in the current version of the TPS. For safety purposes, the TPS places a default ceiling density of 2.25 g/cc when performing CT-to-material mapping. The GBBS

reports dose-to-water by multiplying the GBBS calculated total scalar photon fluence with the mass-energy transfer coefficient for water and summing the results for all energy groups.

Dwell positions and weights were set to mimic 15-10-10 and 15-15 mgRaEq loading for plans with medium and large colpostat models. The cases with small colpostat models mimicked 10-10 mgRaEq loading. Dwell times were determined by calculating a mean dose of 6 Gy to point A using vendor supplied TG-43 parameters (12, 16).

Doses were reported for the following clinical parameters: Manchester A and B, ICRU bladder and rectum, three and nine o'clock, D_{2cc} rectum, D_{2cc} bladder, and D_{2cc} sigmoid. Three and nine o'clock are located on the lateral colpostat surface and represent the patient's left and right vaginal mucosa, respectively. Dose was also reported for the balloon center, but this is not a clinical parameter. DVHs were calculated over the entire contoured volumes.

GBBS Calculations

GBBS calculations are listed in Table 1. Four variables were used in the calculations: solid model applicator, body or patient contour override, rectal and balloon contrast override, and packing contrast override. The calculations have been ordered from ‘least similar to TG-43 phantom’ at the top to ‘most similar to TG-43 phantom’ at the bottom. This ordering is based on material found in the phantom. D(N,M,X,X) is closest to TG-43 since it does not have a solid model applicator and the patient contour from CT is overridden to 1g/cc muscle. D(Y,N,B,B) is furthest from TG-43 because it includes a solid model applicator, uses CT values, and overrides the rectal, balloon, and packing contrast to the densest bone available; this represents a worst case incorrectmapping of contrast material in the TPS. The worst case mapping provides a bound on dosimetric effects that may be caused by variations in the CT numbers of contrast material.

These calculations were performed to 1) isolate factors to clarify differences from TG-43 and 2) determine the sensitivity of mapping contrast materials. For patients not having rectal and sigmoid contrast (patients 4, 5, 12, 14-16, 19, 21, 25) the entire rectum and sigmoid were overridden for D(Y,N,M,M), D(Y,N,B,N), and D(Y,N,B,B). Differences between the GBBS and TG-43 are represented by three factors shown in Table 2: source and boundary, applicator, and tissue heterogeneity. The spatial distribution of each factor is displayed through the patient volume on planes intersecting the applicators.

RESULTS

Figure 1 shows the separation of the three factors spatially for patient two (all patients available in supplement). The source and boundary factor exceeds 10% near the anterior side of the colpostat and is −4% on the posterior surface of the cap. The applicator factor is −3 to −4% on the lateral cap surfaces and a −2% region extends 4 cm laterally. 2-4% increases can be seen along the source tubing in the applicator factor. The source and boundary and applicator factors are generally consistent for all patients. Differences of −4 to −10% can be seen superiorly when the tandem is close to the superior CT edge (patients 2, 17, 18, 23, 26). It can be seen that contrast in the balloon or rectum does not affect the D(Y,N,M,M) calculation. Heterogeneity effects can be seen through air in the rectum with −2% at the anterior rectal wall and over 10% at the posterior wall. For D(Y,N,N,N), the heterogeneity factor is affected by the balloon contrast causing differences over −10% beyond the balloon; this was the case for all patients. The rectal contrast does not significantly change the distribution compared to D(Y,N,M,M). The only difference between D(Y,N,B,B) and D(Y,N,N,N) is that rectal contrast, now being overridden to bone as a worst-case mapping, affects the distribution by about −7%.

Figure 2a shows the three factors contributing to D(Y,N,N,N) at the ICRU rectal point. The source and boundary contribution varies from −0.5% to +2.5%. The applicator contribution varies from about −1% to −2% and the heterogeneity factor varies from − 3.5% to +1.5%. Figure 2b shows the three factors at the balloon center, which is not a clinical parameter (all points are available in the supplement). The contribution of the heterogeneity factor at the balloon center, as expected for D(Y,N,N,N), is dominant due to the incorrect mapping of contrast to bone.

Although differences from TG-43 throughout the patient volume range from −10% to +10%, differences in clinical dosimetric parameters between the GBBS with a solid model applicator and TG-43 are within 3% (A left, A right, B left, B right, D_{2cc} bladder) or 5% (3 o'clock, 9 o'clock, ICRU bladder, ICRU rectum, D2cc rectum, D2cc sigmoid) for all but one calculation. This calculation was the worst case incorrect mapping of contrast to bone D(Y,N,B,B). Differences for this worst case exceeded 5% at ICRU rectum (patients 1 (−6.3%), 4 (−8.5%), 6 (−7.1%),14 (−6.0%), 19 (−6.5%), 21 (−7.5%)), D_{2cc} rectum (patient 4 (−8.1%), 6 (−7.6%), 19 (−5.7%)), and D_{2cc} sigmoid (patient 4 (−5.5%)). Figure 3a shows different heterogeneity factors for different contrast-to-material mappings for the ICRU rectum. When moving from D(Y,N,B,B) to D(Y,N,B,M) the heterogeneity factor changes substantially for the affected patients. This indicates that the incorrect mapping of the packing is responsible for changes in rectal parameters.

The difference in heterogeneity factors between D(Y,N,N,N) and D(Y,N,M,M) is less than 2% for all patients for all clinical parameters. If one is only interested in current clinical parameters and not the entire dose volume, this suggests that overriding contrast to muscle is not necessary.

DISCUSSION

Differences in clinical dosimetric parameters between the GBBS and TG-43 were less than 5% for D(Y,N,N,N) indicating the GBBS has minimal impact on clinical parameters. Incorrect CT-to-material mapping of radiopaque packing to bone has the potential to introduce differences > 5% from TG-43. This was seen when overriding the radiopaque packing to the densest bone possible. Incorrect mapping of rectal and balloon contrast did not impact clinical parameters. However, if one is interested in a more accurate calculation throughout the volume then it is clear from Fig. 1 and Fig. 3b that contrast should be overridden to muscle given that the attenuation of iodine and barium sulfate contrast is closer to muscle than bone (Fig e3a).

Previous work (12) comparing TG-43 with both MC and GBBS for a single source in water showed that both MC and GBBS calculated doses were less (−3 to −5%) than TPS-calculated TG-43 doses within 1 cm of the source just off the longitudinal axis distal to the cable. Our source and boundary factor (Fig 1a) results are in agreement with the previous finding. Furthermore, all the source model differences from TG-43 can be explained by the previous work.

Differences of −7% were seen near the superior edge due to loss of backscatter. Since 3D heterogeneity based calculations are new to brachytherapy, some of the tools available in external beam such as extending the patient boundary past the end of the CT to ensure sufficient backscatter are not yet available. Further investigation on the impact of the superior boundary for a single patient found that it impacted all points by less than 1% except for the B points which were affected by 4% (Fig. f1). Differences in backscatter superior to the tandem were similar to published data (9).

The GBBS returns dose as kerma-to-water in medium ($K_{w,m}$), but kerma-to-medium in medium ($K_{m,m}$) may be the preferred method in the future(17). Calculating dose to a single material, such as water, provides the benefit of smoothing the dose distribution. As can be seen in the supplement, the reporting of dose-to-water is much less sensitive than dose-to-medium. In the cases studied here the difference in $K_{m,m}$ and $K_{w,m}$ is approximately as follows: iodinated contrast 35%, barium sulfate 12%, bone 6%, air −10% (Fig e2 and e3). The nonuniformity of dose-to-medium distribution may make recorded point doses more sensitive to placement, (e.g. accidentally placing a point in contrast would introduce +12% error assuming barium sulfate, +6% for bone, or −10% assuming air). If there is contrast within the rectum or bladder, then recording D_{2cc} to the entire organ instead of the wall could introduce unacceptable errors of over 10% (Fig e4).

With the introduction of 3D heterogeneity-based dose calculations, clinical users should evaluate imaging procedures to determine the accuracy of CT-to-material segmentation. Issues arising from mapping are identical to those seen with MC-based calculations for external photon and electron beam TPSs (18). Incorrect CT-to-material conversion may produce errors in the resulting dose distributions. Such mapping errors occurred in this study when contrast was incorrectly mapped to bone or cartilage for D(Y,N,N,N), but the mapping errors did not impact clinical parameters.

Although the clinical parameters were found to be unaffected by the contrast mapping for D(Y,N,N,N), doses beyond the contrast materials were affected (Fig 1b). The TPS does not include contrast materials, so Monte Carlo simulations were compared to the GBBS to estimate errors. Estimated errors to doses beyond barium sulfate and iodinated contrast mapped to 2.25 g/cc bone are −12% and −9% respectively (Fig e3a). Mapping barium sulfate and iodinated contrast to 1g/cc muscle introduces errors of +1% and +4% respectively. Mapping the iodinated contrast to 1.475 g/cc bone would decrease errors to −2%.

Kwan et al. reported anterior wall measurement differences of −13% and posterior wall differences of +22% when comparing values from an empty and a full rectum for a single source (5). The measured dose differences encountered in our investigation due to heterogeneities were at most −3% to the anterior wall and greater than +10% to the posterior wall. The use of multiple sources and differences in geometry are likely responsible for the difference in magnitude of results.

Library applicators are convenient, but their models in the TPS represent a potential source of error. For model-based dose calculation algorithms such as the GBBS, the independent verification of applicator models in TPS libraries has been an area of concern (17, 19). Some work (20) has been done on validating the TPS's right-sided medium unshielded CT/MR colpostat and is available in the supplement (Fig g2).

The largest limitation in this study was the lack of a control. Although previous studies comparing the GBBS with MC (11-15) and supplemental data comparing GBBS and MC for different materials (Fig e3) provide some level of confidence in our results, a MC simulation for each patient would be ideal. Patient-specific MC was not performed because of the length of time that the setup and running of simulations would have required.

To conclude, the GBBS has minimal impact on clinical parameters. The incorrect CT-to-material mapping of rectal and balloon contrast does not have a significant impact on clinical parameters. Rectal parameters may be sensitive to the CT-to-material mapping of radiopaque packing.

Supplementary Material

Refer to Web version on PubMed Central for supplementary material.

Acknowledgments

The authors thank Sophie Wetherall from Varian Medical Systems for providing further details on the BrachyVision TPS.

Supported in part by the National Institutes of Health through grant 2R44CA105806-02 and MD Anderson's Cancer Center Support Grant CA016672.

This study investigated the use of a grid-based Boltzmann solver (GBBS) for cervical cancer patients treated with an unshielded CT/MR applicator. The GBBS was found to have minimal impact on clinical dosimetric parameters for the cohort of GYN patients. GBBS differences from TG-43 for the clinical parameters were mainly due to source, boundary, and applicator model differences. CT-to-material mapping of rectal and balloon contrast does not matter for clinical parameters. Rectal parameters may be affected by incorrectly mapping packing material.

REFERENCES

1. Viswanathan AN, Erickson BA. Three-dimensional imaging in gynecologic brachytherapy: a survey of the American Brachytherapy Society. Int J Radiat Oncol Biol Phys. 2010; 76:104–109. [PubMed: 19619956]
2. Rivard MJ, Coursey BM, DeWerd LA, et al. Update of AAPM Task Group No. 43 Report: A revised AAPM protocol for brachytherapy dose calculations. Med Phys. 2004; 31:633–674. [PubMed: 15070264]
3. Poon E, Williamson JF, Vuong T, et al. Patient-Specific Monte Carlo Dose Calculations for High-Dose-Rate Endorectal Brachytherapy With Shielded Intracavitary Applicator. Int J Radiat Oncol Biol Phys. 2008; 72:1259–1266. [PubMed: 18954720]
4. Richardson S, Palaniswaamy G, Grigsby PW. Dosimetric effects of air pockets around high-dose rate brachytherapy vaginal cylinders. Int J Radiat Oncol Biol Phys. 2010; 78:276–279. [PubMed: 20395068]
5. Kwan IS, Wilkinson D, Cutajar D, et al. The effect of rectal heterogeneity on wall dose in high dose rate brachytherapy. Med Phys. 2009; 36:224–232. [PubMed: 19235390]
6. Price MJ, Kry SF, Eifel PJ, et al. Dose perturbation due to the polysulfone cap surrounding a Fletcher-Williamson colpostat. J Appl Clin Med Phys. 2010; 11:3146. [PubMed: 20160700]
7. Meigooni AS, Nath R. Tissue inhomogeneity correction for brachytherapy sources in a heterogeneous phantom with cylindrical symmetry. Med Phys. 1992; 19:401–407. [PubMed: 1584139]
8. Poon E, Verhaegen F. A CT-based analytical dose calculation method for HDR ^{192}Ir brachytherapy. Med Phys. 2009; 36:3982–3994. [PubMed: 19810471]
9. Melhus CS, Rivard MJ. Approaches to calculating AAPM TG-43 brachytherapy dosimetry parameters for ^{137}Cs, ^{125}I, ^{192}Ir, ^{103}Pd, and ^{169}Yb sources. Med Phys. 2006; 33:1729–1737. [PubMed: 16872080]
10. Nag S, Cardenes H, Chang S, et al. Proposed guidelines for image-based intracavitary brachytherapy for cervical carcinoma: Report from Image-Guided Brachytherapy Working Group. International Journal of Radiation Oncology*Biology*Physics. 2004; 60:1160–1172.
11. Zourari K, Pantelis E, Moutsatsos A, et al. Dosimetric accuracy of a deterministic radiation transport based ^{192}Ir brachytherapy treatment planning system. Part I: single sources and bounded homogeneous geometries. Med Phys. 2010; 37:649–661. [PubMed: 20229874]
12. Mikell JK, Mourtada F. Dosimetric impact of an ^{192}Ir brachytherapy source cable length modeled using a grid-based Boltzmann transport equation solver. Medical Physics. 2010; 37:4733–4743. [PubMed: 20964191]
13. Petrokokkinos L, Zourari K, Pantelis E, et al. Dosimetric accuracy of a deterministic radiation transport based [sup 192]Ir brachytherapy treatment planning system. Part II: Monte Carlo and

experimental verification of a multiple source dwell position plan employing a shielded applicator. Medical Physics. 2011; 38:1981–1981. [PubMed: 21626931]

14. Gifford KA, Price MJ, Horton JL Jr. et al. Optimization of deterministic transport parameters for the calculation of the dose distribution around a high dose-rate ^{192}Ir brachytherapy source. Med Phys. 2008; 35:2279–2285. [PubMed: 18649459]
15. Gifford KA, Wareing TA, Failla G, et al. Comparison of a 3-D multi-group SN particle transport code with Monte Carlo for intracavitary brachytherapy of the cervix uteri. J Appl Clin Med Phys. 2010; 11:3103. [PubMed: 20160682]
16. Angelopoulos A, Baras P, Sakelliou L, et al. Monte Carlo dosimetry of a new ^{192}Ir high dose rate brachytherapy source. Med Phys. 2000; 27:2521–2527. [PubMed: 11128304]
17. Rivard MJ, Beaulieu L, Mourtada F. Enhancements to commissioning techniques and quality assurance of brachytherapy treatment planning systems that use model-based dose calculation algorithms. Medical Physics. 2010; 37:2645–2658. [PubMed: 20632576]
18. Chetty IJ, Curran B, Cygler JE, et al. Report of the AAPM Task Group No. 105: Issues associated with clinical implementation of Monte Carlo-based photon and electron external beam treatment planning. Med Phys. 2007; 34:4818–4853. [PubMed: 18196810]
19. Hellebust TP, Kirisits C, Berger D, et al. Recommendations from Gynaecological (GYN) GEC-ESTRO Working Group: Considerations and pitfalls in commissioning and applicator reconstruction in 3D image-based treatment planning of cervix cancer brachytherapy. Radiotherapy and Oncology. 2010; 96:153–160. [PubMed: 20663578]
20. Mikell J, Mourtada F. Monte Carlo Verification of a CT/MR Ovoid Model Used by a Grid-Based Boltzmann Solver in a Commercial Treatment Planning System. Brachytherapy. 2011; 10:S36.

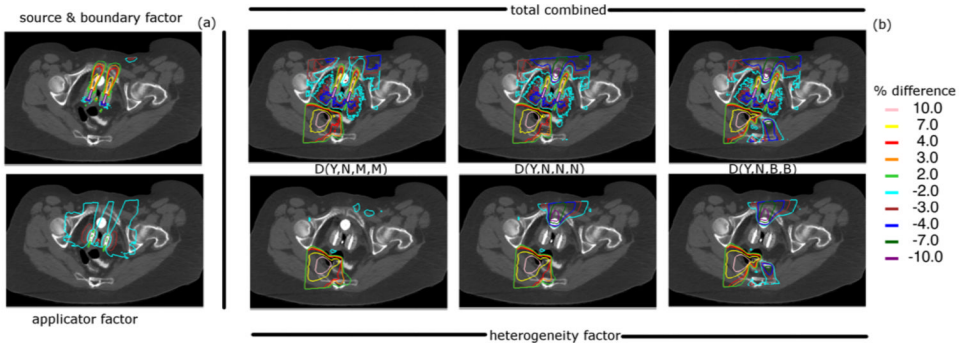

Figure 1.

Spatial distributions of the 3 factors contributing to differences between GBBS and TG-43: source and boundary, applicator, and heterogeneity. The contrast is overridden to muscle, no override, or bone. **(a)** Top: contribution of source and boundary. Bottom: contribution of applicator. **(b)** Top row: combination of all three factors. Bottom row: contribution of the heterogeneity. From left to right, the GBBS with solid applicator with contrast overridden to muscle D(Y,N,M,M), contrast not overridden D(Y,N,N,N), or contrast overridden to bone D(Y,N,B,B).

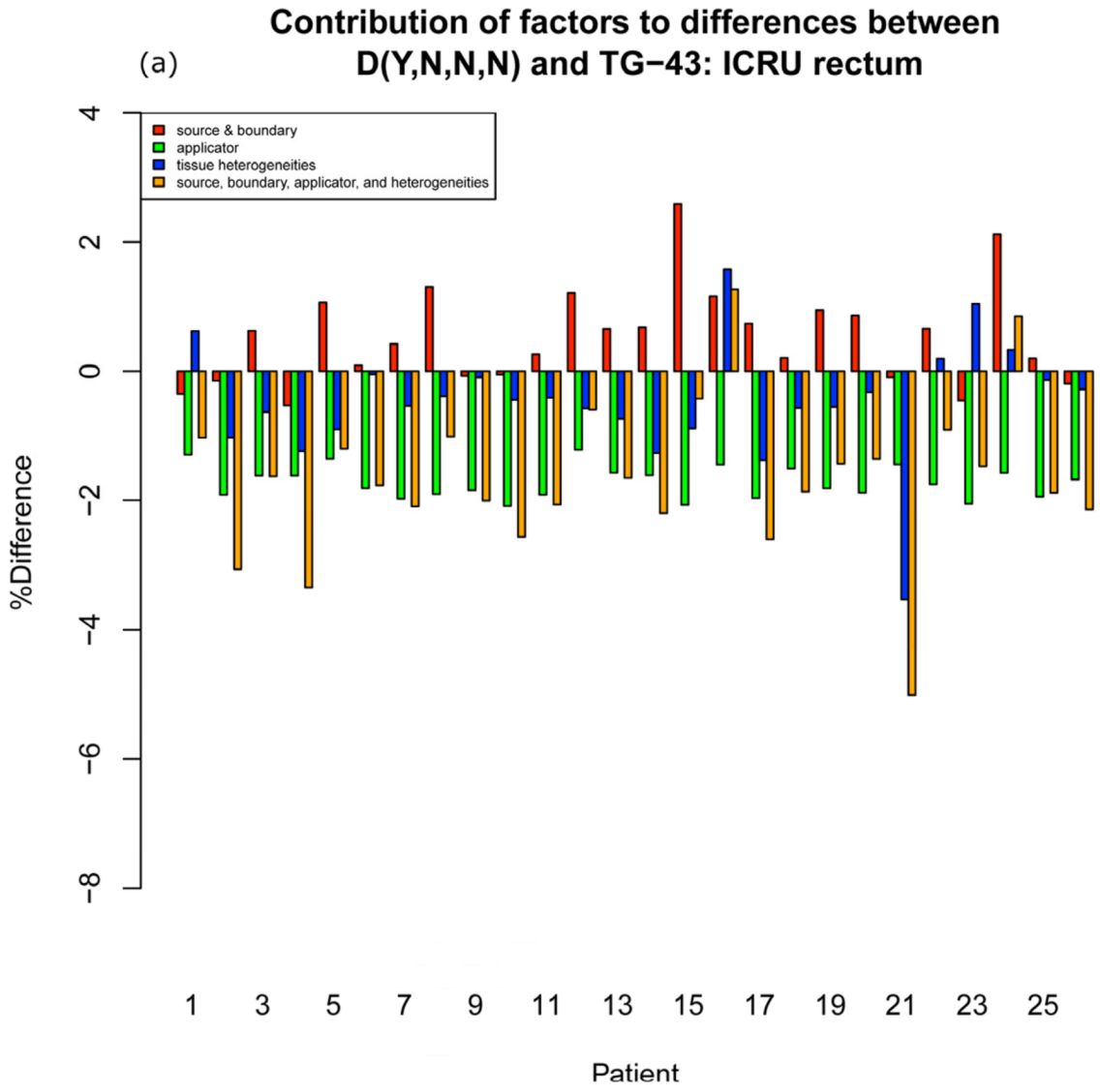

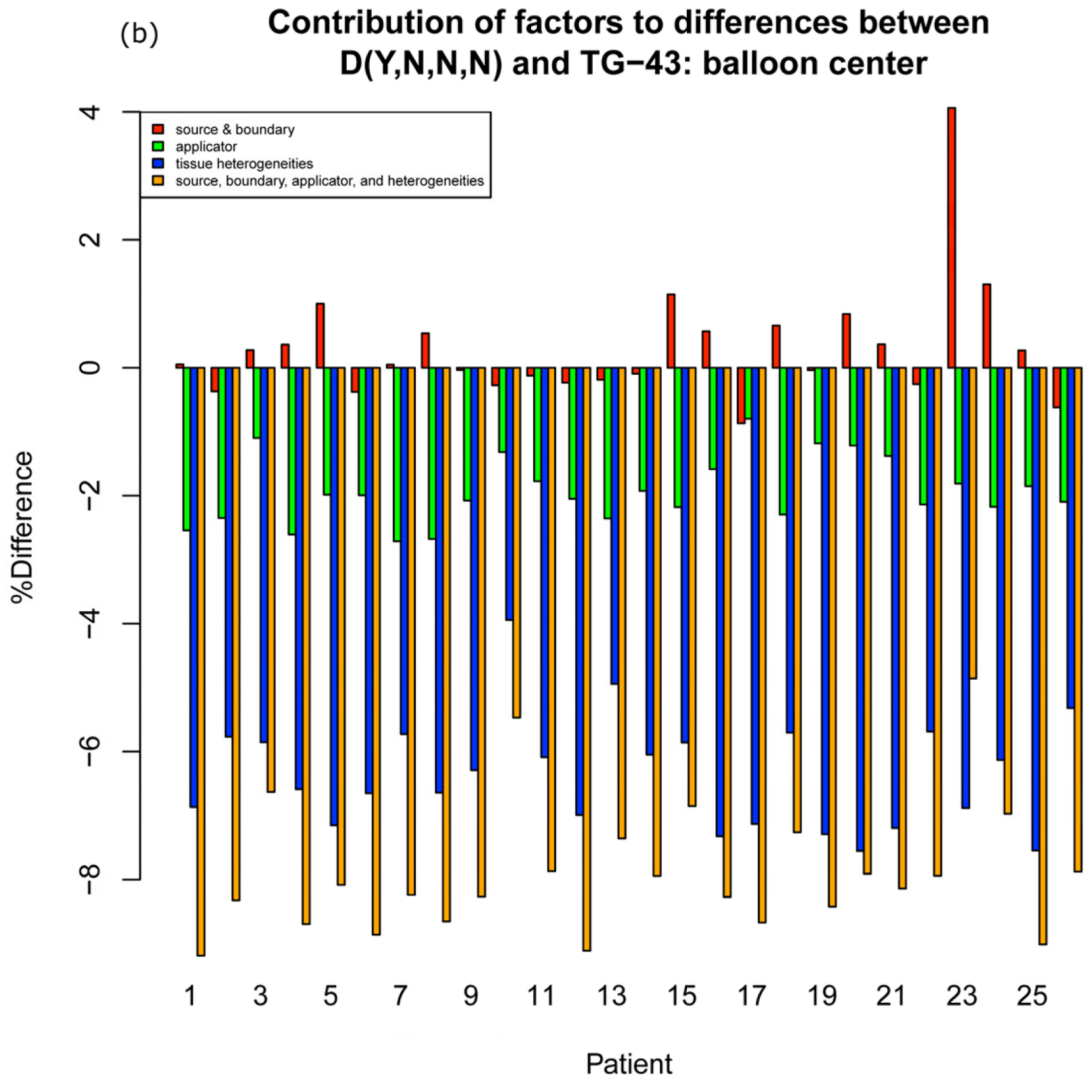

Figure 2.

Barplots showing contribution of factors to differences between the GBBS with solid applicator and no overrides D(Y,N,N,N) and TG-43. Summing source and boundary (red), applicator (green), and tissue heterogeneities (blue) yields the total percent difference (orange) from TG-43. **(a)** ICRU rectum **(b)** balloon center

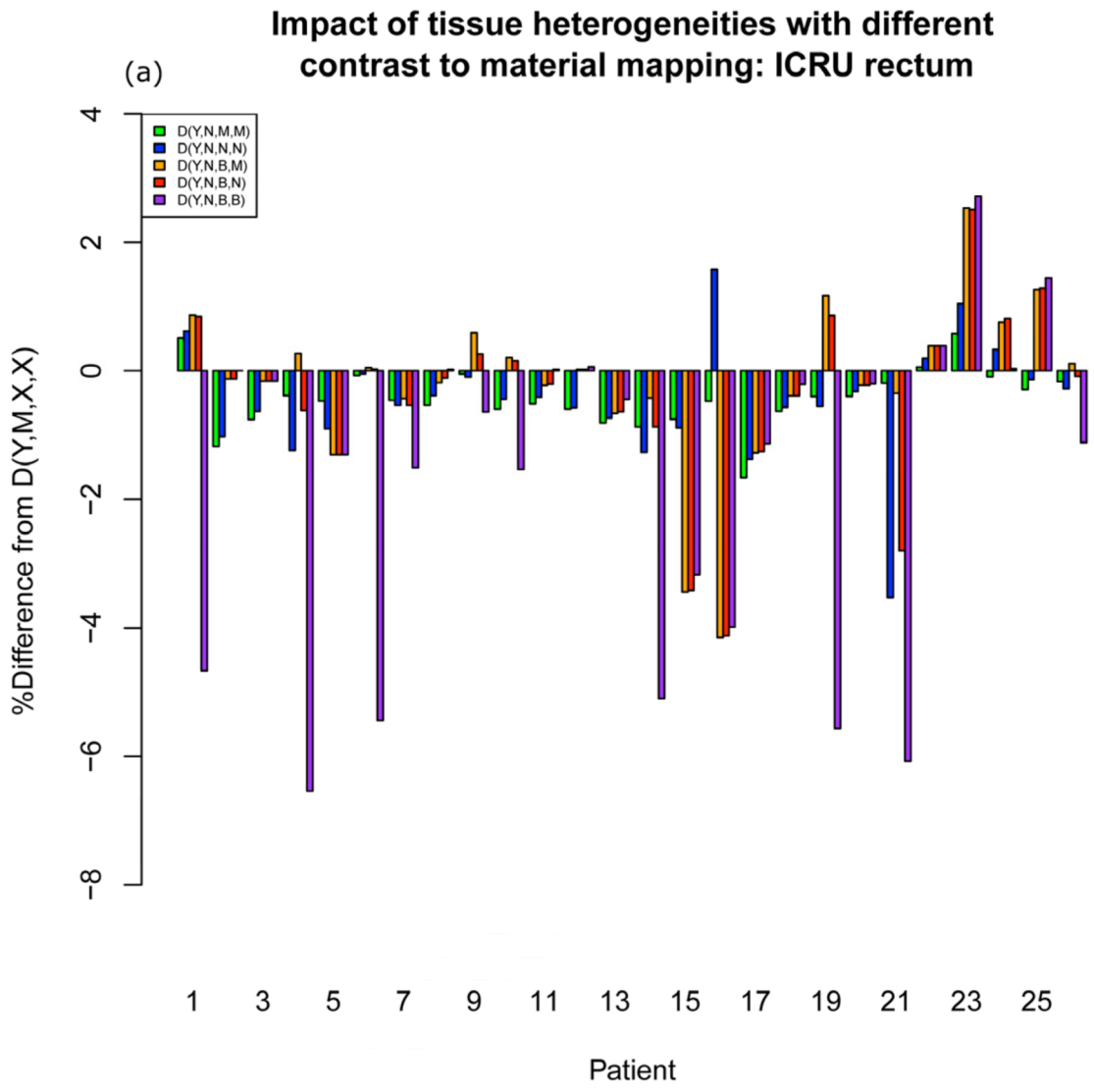

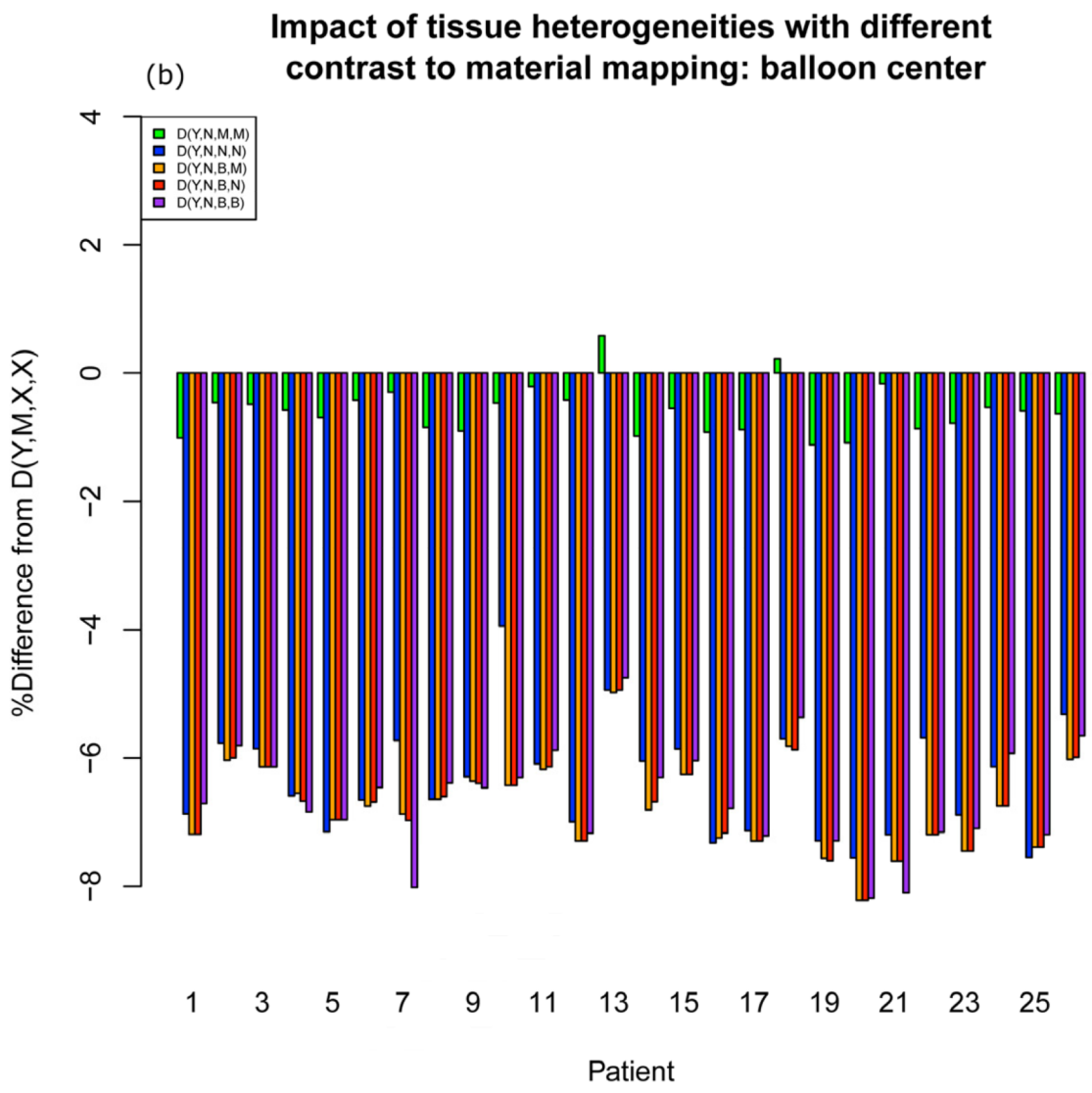

Figure 3.
Barplots showing different heterogeneity factors for different contrast-to-material mappings at **(a)** ICRU rectum **(b)** balloon center

Table 1

Summary of different GBBS calculations.

GBBS calculation	Applicator	Body override	Rectal and balloon contrast	Packing contrast override
D(Y, N, B, B)	Y	N	B	B
D(Y, N, B, N)	Y	N	B	N
D(Y, N, B, M)	Y	N	B	M
D(N, N, N, N)	N	N	N	N
D(Y, N, N, N)	Y	N	N	N
D(Y, N, M, M)	Y	N	M	M
D(Y, M, X, X)	Y	M	X	X
D(N, M, X, X)	N	M	X	X

Four variables were used in the GBBS calculations. D(solid applicator, body override, rectal and balloon override, packing override). Y = yes solid applicator was used, N = no solid applicator was used or no override was specified. B denotes that the contour was overridden to 2.25 g/cc bone. M denotes that the contour was overridden to 1g/cc muscle. X denotes that the value of the contour is not applicable since a larger contour is overriding its value.

Table 2

Factors contributing to differences between the GBBS and TG-43

total difference = source & boundary factor × applicator factor × heterogeneity factor

$$\frac{D(Y,N,N,N)}{TG43} = \frac{D(N,M,X,X)}{TG43} \times \frac{D(Y,M,X,X)}{D(N,M,X,X)} \times \frac{D(Y,N,N,N)}{D(Y,M,X,X)}$$

Factor	TG-43	GBBS	Quantity that isolates factor
Source and boundary model	15 cm cable on source and 30 cm diameter sphere	1 mm cable on source and patient boundaries from CT	D(N,M,X,X)/TG-43
Applicator model	None	Solid model applicator from library	D(Y,M,X,X)/D(N,M,X,X)
Heterogeneity model	None	CT-to-material mapping includes air, lung, adipose, muscle, cartilage, and bone.	D(Y,N,N,N)/D(Y,M,X,X)